

# Gliolectin-mediated carbohydrate binding at the *Drosophila* midline ensures the fidelity of axon pathfinding

Mary Sharrow and Michael Tiemeyer\*

Department of Cell Biology, Yale University School of Medicine, 333 Cedar St, New Haven, CT 06510, USA

\*Author for correspondence (e-mail: mtiemeyer@glyko.com)

Accepted 16 August 2001

## SUMMARY

Gliolectin is a carbohydrate-binding protein (lectin) that mediates cell adhesion *in vitro* and is expressed by midline glial cells in the *Drosophila melanogaster* embryo. Gliolectin expression is maximal during early pathfinding of commissural axons across the midline (stages 12-13), a process that requires extensive signaling and cell-cell interactions between the midline glia and extending axons. Deletion of the *gliolectin* locus disrupts the formation of commissural pathways and also delays the completion of longitudinal pathfinding. The disruption in commissure formation is accompanied by reduced axon-glial contact, such that extending axons grow on other axons and form a tightly fasciculated bundle that arches over the midline. By contrast, pioneering commissural axons normally cross the midline as a distributed array of fibers that interdigitate among the midline glia, maximizing contact and, therefor,

communication between axon and glia. Restoration of Gliolectin protein expression in the midline glia rescues the observed pathfinding defects of null mutants in a dose-dependent manner. Hypomorphic alleles generated by ethylmethanesulfonate mutagenesis exhibit a similar phenotype in combination with a deletion and these defects are also rescued by transgenic expression of Gliolectin protein. The observed phenotypes indicate that carbohydrate-lectin interactions at the *Drosophila* midline provide the necessary surface contact to capture extending axons, thereby ensuring that combinatorial codes of positive and negative growth signals are interpreted appropriately.

Key words: Carbohydrate, Lectin, Axon pathfinding, Glia, *Drosophila*

## INTRODUCTION

The formation of a functioning nervous system requires that axons extend along appropriate pathways to reach correct terminal fields during embryonic development. Axon pathfinding in a broad range of organisms is characterized by the ability of neuronal growth cones to discriminate between appropriate and inappropriate growth substrates (Bovolenta and Mason, 1987; Landmesser et al., 1990; Marcus et al., 1995; Stoeckli and Landmesser, 1998; Stoeckli et al., 1997). In *Drosophila*, such discrimination is especially evident at choice points where the consequences of continued extension versus axon redirection generate distinct morphologic structures (Isbister et al., 1999; Jacobs and Goodman, 1989a; Jacobs and Goodman, 1989b; Kolodkin et al., 1992). For example, partitioning of the total *Drosophila melanogaster* embryonic axon pool either into commissural bundles that cross the midline or into longitudinal processes that grow in the anterior-posterior direction creates a characteristic orthogonal axon scaffold (Klämbt and Goodman, 1991a; Klämbt and Goodman, 1991b; Klämbt et al., 1991).

The function of a population of glial cells at the *Drosophila* embryonic midline (midline glial cells) is crucial to the guidance and organization of commissural and longitudinal fibers (Hummel et al., 2000; Hummel et al., 1999). Signals

originating from the midline glia allow commissural axons to cross the midline and keep longitudinal axons away from the midline (Harris et al., 1996; Seeger et al., 1993; Stein and Tessier-Lavigne, 2001). Both the amount (dose) and the type (molecular identity) of signaling can determine growth cone behavior, dictating the co-requisite establishment of an axon-glia interface that facilitates high-fidelity transmission of molecular signals (Kidd et al., 1998b; Winberg et al., 1998). While the identities and functions of relevant signaling molecules and receptor families have been elegantly described, comparatively little progress has been made towards understanding whether additional components of the neuronal and midline glial cell surfaces contribute to signal transmission by regulating the axon-glia interface.

At the very least, it may be necessary for exploring growth cones to adhere to the midline glial surface before sufficient signal integration or sorting ensures that the maturing axon is appropriately routed. Among *Drosophila* molecules that mediate cell adhesion, only the Gliolectin protein is expressed in midline glia, coincident with the extension of commissural and longitudinal axon pathways (Tiemeyer and Goodman, 1996). Originally identified in an adhesion-based cloning screen for embryonically expressed carbohydrate-binding proteins (lectins), Gliolectin binds a subset of N-acetylglucosamine-terminated *Drosophila* glycans. That a

lectin-carbohydrate interaction might contribute to the initial contact between axons and midline glia is consistent with demonstrated and proposed functions of carbohydrate-mediated cell adhesion in other contexts.

The tissue, cell-type and developmental specificity of glycan expression has engendered proposals that cell-surface oligosaccharides function as recognition ligands. The characterization of *Drosophila* glycans is still in its infancy but so far indicates complexity sufficient to support cell-specific expression comparable to that of other organisms (Callaerts et al., 1995; D'Amico and Jacobs, 1995; Fredieu and Mahowald, 1994; Fristrom and Fristrom, 1982; Rietveld et al., 1999; Roth et al., 1992; Seppo et al., 2000; Seppo and Tiemeyer, 2000; Toyoda et al., 2000). We have therefore investigated whether loss of Gliolectin generates phenotypes indicative of aberrant cell-recognition at the midline. We find that loss of Gliolectin affects the efficiency but not the specificity of pathfinding. While gross alterations in the architecture of the axon scaffold are apparent, commissures and longitudinals still form in the absence of Gliolectin. The results are consistent with a need for carbohydrate-mediated axon capture at the midline that initiates and facilitates subsequent signaling between axon and glia. We propose that specific axon pathfinding across the midline emerges from combining axon capture, which may be largely indiscriminate, with subsequent signal transmission.

## MATERIALS AND METHODS

### Reagents

Monoclonal antibodies 1D4, BP102 and 22C10 were kindly provided by Corey Goodman (University of California at Berkeley). The anti-Gliolectin monoclonal antibody designated 1B7 was originally generated in the Goodman laboratory but is now maintained by the authors (Tiemeyer and Goodman, 1996). Secondary antibodies were obtained from Jackson Laboratories (Westgrove, PA). Other reagents were of the highest purity obtainable from standard sources.

### Fly stocks

The *rhomboid*-Gal4 line,  $w^-$ ; *rho*-Gal4/*rho*-Gal4, was obtained from Tian Xu, Yale University. The *Gliolectin* null line  $Df(3R)e^{-BS2}$ , *rsd*<sup>1</sup>/TM3 (the deletion chromosome is designated  $\Delta 3013$ ) and all other stocks were acquired from the Bloomington Stock Center (Bloomington, IN). For generation of UAS-*gliolectin* (UAS-*glec*) transformant lines, a *Xho*I fragment, containing the entire Gliolectin-coding sequence, was cut from subclone NH3-2/19 in pCDM8 and ligated into pBluescript (Tiemeyer and Goodman, 1996). Subcloned plasmid bearing Gliolectin insert in the appropriate orientation was then digested with *Not*I and *Kpn*I, and the resulting Gliolectin fragment was ligated into the pUAST3 vector previously cut with the corresponding enzymes (Brand et al., 1994). Injection of the resulting construct, designated pUAST3*glec*, into  $w^{1118}$  flies and the generation of transformant lines were achieved using standard procedures.

### Immunohistochemistry

Embryo collections were dechorionated, fixed and devitellinized according to standard methods (Patel, 1994). Because decreased 1B7 (anti-Gliolectin) staining was observed in embryos stored for extended periods (> 1 month) in methanol at  $-20^{\circ}\text{C}$ , embryos were routinely processed for staining within 2 weeks of preparation. After two 10 minute washes in PBT (0.3% w/v Triton X-100 in phosphate-buffered saline (PBS)), embryos were blocked for 30 minutes in PBT containing 0.1% w/v bovine serum albumin and 5% normal goat serum at room temperature. Dilutions of primary antibody in the same

solution were then substituted for blocking solution and the embryos were incubated at  $4^{\circ}\text{C}$  overnight. Primary antibody was washed out with four 10 minute washes in PBT at room temperature. After reblocking for 15 minutes, embryos were incubated at room temperature for 3 hours in horseradish peroxidase (HRP)-conjugated goat anti-mouse secondary antibody diluted 1:500. After washing out the secondary antibody, HRP activity was detected by precipitation of DAB (3-3' diaminobenzidine, 0.3 mg/ml in PBT) in the presence of  $\text{H}_2\text{O}_2$  (0.03% w/v). After 15 minutes in the detection reagent, embryos were washed and subsequently cleared by settling through 50%, then 70% glycerol in PBS. In those cases where the DAB reaction product was nickel enhanced,  $\text{NiCl}_2$  (0.64% w/v final concentration) was added prior to the addition of  $\text{H}_2\text{O}_2$ . Primary antibody dilutions were 1:5 for 1B7, 1:3 for BP102 and 1:50 for 1D4. After staining, embryos were staged as whole mounts and then dissected using tungsten needles before photomicroscopy.

For frozen sections, stained embryos were equilibrated overnight in SPT (25% w/v sucrose, 0.03% w/v Triton X-100 in PBS) immediately after the detection reaction. After staging as whole mounts, the desired embryos were segregated and pipetted in 20  $\mu\text{l}$  total volume of SPT into the top 25% of a small volume (approximately 200  $\mu\text{l}$ ) of TBS Tissue Freezing Medium (Electron Microscopy Sciences) in a 1.5 ml eppendorf centrifuge tube. As the embryos sank through the mounting media, they oriented themselves vertically along their anterior-posterior axis. Once the embryos were sufficiently aligned, the entire centrifuge tube was quick frozen in crushed dry ice. The conical part of the centrifuge tube was then clipped just above the position of the embryos, releasing a small, frozen cone of mounting media (approximately 100  $\mu\text{l}$ ) containing the aligned embryos. After attachment to a cryostat chuck, serial 20  $\mu\text{m}$  sections through multiple segments of multiple wild-type and  $\Delta 3013/\Delta 3013$  embryos were collected on clean glass slides. After drying overnight at room temperature, the sections were coverslipped under 50% glycerol before photomicroscopy.

Embryo staging is as described by Campos-Ortega (Campos-Ortega and Hartenstein, 1997) as modified by Klämbt (Klämbt and Goodman, 1991b). Stages 12/5 through 12/0 were identified by the number of segments remaining on the dorsal side of the retracting germ band. Stage 13 was judged to be early when the amnioserosa was completely unfolded, the clypeolabrum was extremely thin and the hindgut had not yet assumed a sigmoidal shape. The stages from mid-13 to early 14 were distinguished by the formation of the dorsal ridge, by the extent of the dorsal expansion of the lateral ectoderm, and by the morphology of the hindgut and of the maxillary, mandibular and labial segments.

In rescue experiments, multiple landmarks were used to distinguish transgenic embryos lacking endogenous Gliolectin (UAS-*glec*<sup>+</sup>; *rho*-Gal4<sup>+</sup>;  $\Delta 3013/\Delta 3013$ ) from those that carried a functional copy of the *glec* gene (supplied by the balancer chromosome). By mid-stage 13, *Rho* drives expression in mesodermal and ectodermal cells that do not normally express Gliolectin protein (Bier et al., 1990). In addition to the midline glia of the ventral nerve cord, Glec protein is also normally expressed by a subset of cells in the supraesophageal ganglia. Therefore, absence of 1B7 staining in the head, accompanied by staining of all midline glia and additional ectodermal and mesectodermal cells indicates transgenic Gliolectin expression in a *Glec*-null embryo. When embryos were double stained for both Gliolectin expression (1B7) and an axonal marker (1D4 or BP102), it was necessary to nickel enhance the axonal marker (black) so that it could be clearly distinguished above the 1B7 midline staining.

### Generation of rescue lines

Transformation with the pUAST3*glec* vector yielded UAS-*glec* insertions on both the X (line 8-19) and second chromosomes (line 10-9). To introduce the UAS-*glec* element into the *gliolectin* null background, the  $\Delta 3013$  deletion line was first crossed to  $w^-$ ; *D,ry*/TM3 to put the deficiency into a  $w^-$  background. The resulting

$w^-$ ;  $\Delta 3013/TM3$  stock was crossed to the UAS-*glec* insertion line 8-19 to create a UAS-*glec*;  $\Delta 3013/TM3$  stock. Similarly,  $w^-$ ; *rho-Gal4/rho-Gal4* (*rhomboid-Gal4*) flies were crossed to  $\Delta 3013$  to create  $w^-$ ; *rho-Gal4/+*;  $\Delta 3013/TM3$  stocks. It was not possible to generate flies homozygous for *rho-Gal4* in this background. Single-copy rescue was assessed by collecting embryos from a cross of UAS-*glec*;  $\Delta 3013/TM3$  females to  $w^-$ ; *rho-Gal4/+*;  $\Delta 3013/TM3$  males. For double-copy rescue, a UAS-*glec*; UAS-*glec*;  $\Delta 3013/TM3$  stock was generated from UAS-*glec* insertion lines bearing elements on the X (line 8-19) and second chromosomes (line 10-9).

**Generation of EMS mutants**

Male  $w^{1118}$  flies ( $n=50$ ) were treated with ethylmethanesulfonate (EMS) according to standard methods (Lewis and Bacher, 1988). Mutagen-treated males were mated to virgin  $w^-$ ; *D,ry/TM3* females. Single male or female  $w^-$ , *Sb^-*, *D^+* progeny were then mated to either  $w^-$ ;  $\Delta 3013/TM3$  or  $w^-$ ;  $\Delta 3013/TM6b$  ( $n=600$ ). Ten of these crosses gave only *Sb^-* (TM3-balanced) or *Hu^-* (TM6b-balanced) progeny, indicating non-complementation of the  $\Delta 3013$  lethality, and were kept for further analysis.

**RESULTS**

**Gliolectin is expressed by midline glia coincident with commissural and longitudinal axon outgrowth**

An anti-Gliolectin monoclonal antibody, designated 1B7, detects Gliolectin expression at the midline of the embryonic ventral nerve cord from stage 12/3 through to early stage 15 (Tiemeyer and Goodman, 1996). Staining is particularly robust in the midline glial cells, MGA and MGM, from stages 12/1 through mid-13, when extending axons pioneer commissural and longitudinal pathways (Fig. 1A). Double-staining with 1B7 and the monoclonal antibody BP102, which recognizes an epitope shared by many CNS axons, demonstrates the intimate association between midline glial cells and commissural fibers as these axons cross the midline during late stage 12 and early stage 13 (Fig. 1B). Embryos homozygous for a chromosomal deletion designated  $\Delta 3013$  (breakpoints 93C6-94A1), lack the *gliolectin* locus (*glec* maps to 93F6-8) and are not stained by monoclonal antibody 1B7 (Fig. 1C).

**Loss of Gliolectin results in defective commissure formation**

In wild-type embryos at late stage 12, neurons that pioneer commissural pathways extend processes that interdigitate amongst the midline glia (Fig. 2A,B). By stage mid-13, coordinated movements of axons and glial cells segregate the commissural mass into distinct anterior and posterior bundles (Fig. 2C-E). By contrast,  $\Delta 3013$  homozygous embryos at stage 12/1 and early 13 form a commissural projection with a distinctively fused or monofilamentous appearance (Fig. 2F,G, arrowheads). The fused commissure phenotype persists later into stage 13 in the deletion homozygote when a pronounced absence of axons in the longitudinal pathways also becomes apparent (Fig. 2H-J, arrow in H). Quantitation of the fused commissure phenotype demonstrates that all deletion homozygote embryos are phenotypically abnormal with, on average, defects in greater than one-half of their segments (Table 1).

The arched appearance of the fused commissures in late stage 12,  $\Delta 3013/\Delta 3013$  embryo dissections (Fig. 2F,G) implies that axons must follow aberrant routes across the midline.

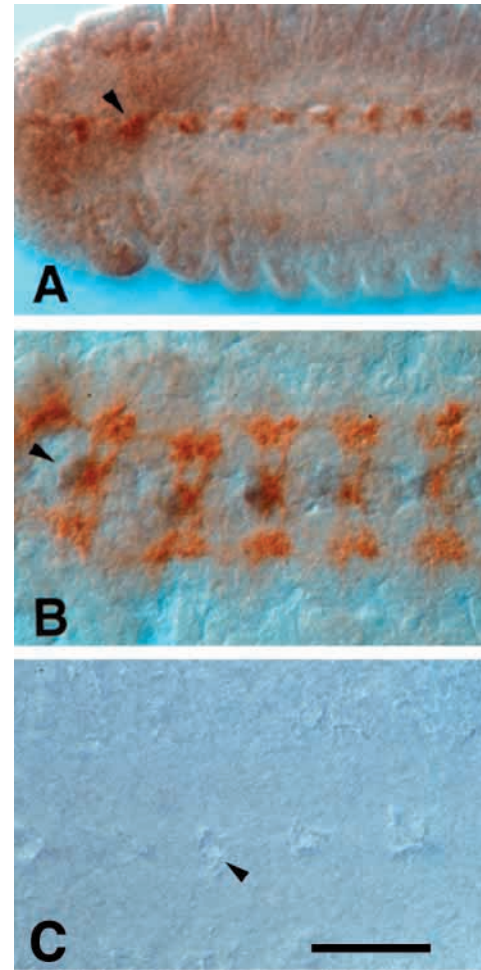


**Fig. 1.** Gliolectin is expressed in the embryonic *Drosophila* nerve cord during commissural and longitudinal pathfinding. Expression of gliolectin in the midline glia at early stage 13. (A) In wild-type embryos, the midline glia stain with the anti-Gliolectin monoclonal antibody 1B7 (arrowhead, ventral view of a whole mount embryo). (B) A wild-type embryo dissected after staining with 1B7 (black) and BP102 (brown) demonstrates the spatial and temporal relation between Gliolectin expression and axon scaffold formation at early stage 13. (C) In  $\Delta 3013$  homozygotes, Gliolectin expression is completely absent at the midline by 1B7 antibody staining (arrowhead). Scale bar: 64  $\mu m$  in A; 25  $\mu m$  in B; 16  $\mu m$  in C.

Thus, transverse sections through the ventral nerve cord reveal that commissural axons form a dense bundle at the dorsal boundary of the nerve cord in deletion homozygotes (Fig. 3C, arrowhead). By contrast, commissural axons interdigitate amongst the midline glia in wild-type embryos (Fig. 3A,B). Furthermore, commissural bundles appear thicker and the longitudinally oriented fibers are sparse in deletion embryos, indicating that commissural accumulation is at the expense of longitudinal mass (Fig. 3, arrows). Although not quantitated, the width of the axon scaffold, as labeled by mAb BP102, is consistently greater in  $\Delta 3013$  homozygotes than in age-matched wild-type embryos at late stage 12 through mid-stage 13 (Fig. 2, Fig. 3). Segmental width is also altered in another mutation affecting axon-glial interactions at the *Drosophila* midline (Seeger et al., 1993), suggesting that the integrity of

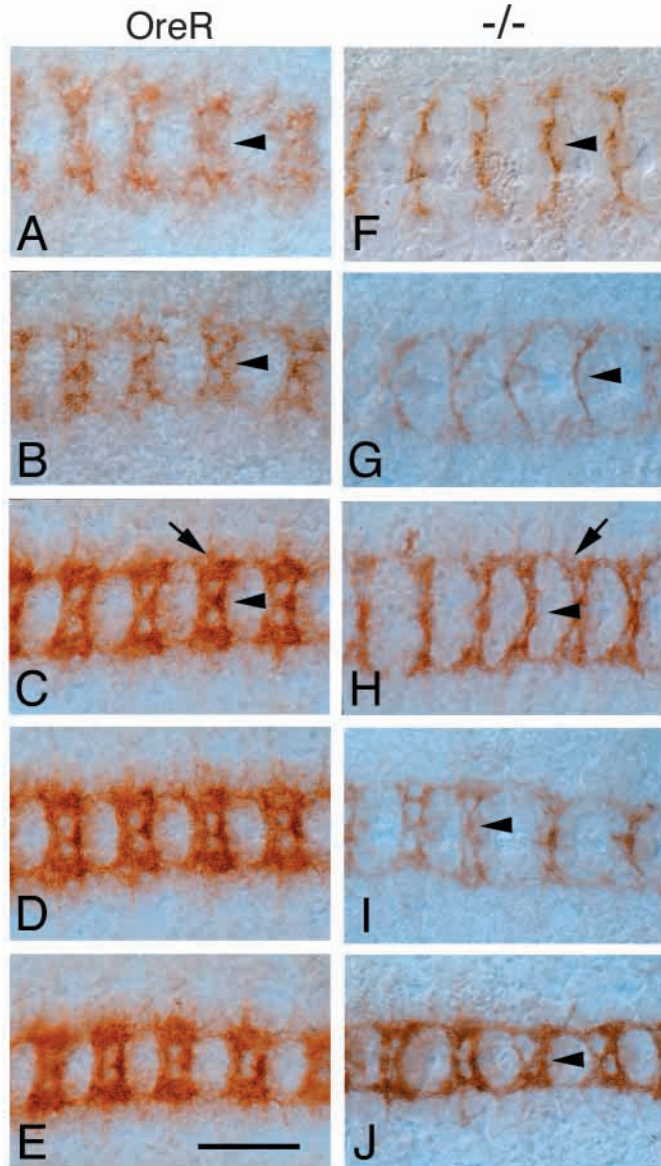


**Fig. 2.** Loss of Gliolectin perturbs commissure formation. BP102 staining of embryos from late stage 12 through late stage 13 (A,F, stage 12/1; B,G, stage early 13; C,H, stage mid 13; D,I, stage late 13; E,J, stage early 14) shows the progressive development of distinct, well separated commissures in wild type (OreR, A-E) and the effects of loss of Gliolectin in  $\Delta 3013$  homozygotes ( $-/-$ , F-J). In OreR embryos at stage 12/1, commissural axons (A, arrowhead) are diffusely spread among the midline glia but by early stage 13 (B, arrowhead) commissural separation is becoming apparent. In  $\Delta 3013$  homozygotes, however, the commissures are tightly fasciculated into a single bundle in late stage 12 and early stage 13 embryos (F,G, arrowhead) and remain poorly separated into mid-stage 13 (H, arrowhead). By mid-stage 13, wild-type commissures (C, arrowhead) have separated into anterior and posterior bundles and the longitudinal pathways (arrow) are evident within each segment. In  $\Delta 3013$  homozygotes at mid-stage 13, the forming longitudinal pathways possess less axon density than wild-type (compare arrows in C and H). Partial commissural fusions and distortions remain common in late-stage 13 and early-stage 14 deletion homozygotes (I,J, arrowheads). Scale bar: 11  $\mu$ m.

segmental CNS architecture builds upon appropriate commissure formation.

The deletion interval in  $\Delta 3013$  encompasses at least 12 other known genes. Therefore, chemical mutagenesis of the *glec* locus was undertaken. EMS mutagenesis yielded ten homozygous lethal lines that failed to complement the lethality of  $\Delta 3013$ . When embryos collected from balanced, non-complementing EMS mutants were stained with BP102, axon pathfinding defects were not apparent. However, when crossed to the  $\Delta 3013$  stock, two EMS lines, *glec*<sup>m24</sup> and *glec*<sup>m98</sup>, both demonstrated fused and disrupted commissural architecture (Fig. 4) although less frequently than in the deletion homozygote (Table 2). Therefore, the EMS-mutagenized chromosomes, *glec*<sup>m24</sup> and *glec*<sup>m98</sup>, fail to rescue the loss-of-function phenotype observed in  $\Delta 3013/\Delta 3013$  embryos.

The two EMS mutants present slightly different phenotypes. In particular, *glec*<sup>m98</sup> is characterized by greater commissural fusion (Fig. 4C,D, arrowheads) and more severe loss of longitudinal mass than in *glec*<sup>m24</sup> (Fig. 4C,D, arrows). Although embryos homozygous for either EMS mutation display no axonal phenotype, the two mutant chromosomes do affect the axon scaffold when combined. Embryos carrying both mutations exhibit commissural distortion, fusion and thinning (Fig. 4E, arrowhead) as well as minimal loss of longitudinal mass (Fig. 4E, arrow). As embryo collections from balanced EMS lines are normal and since the penetrance of the scored phenotypes in the sensitized background (*glec*<sup>m24</sup>/ $\Delta 3013$  or *glec*<sup>m98</sup>/ $\Delta 3013$ ) is intermediate between wild-type and  $\Delta 3013/\Delta 3013$ , both EMS alleles were classified as hypomorphs. However, it is unlikely that the effect of either mutation results solely from decreased gene product as Gliolectin protein is detectable in both EMS mutants, even when placed over the  $\Delta 3013$  chromosome (Fig. 4C,D). In addition, the ability of each EMS mutant to enhance the phenotype of the other suggests a synthetic interaction between altered molecular forms rather than a simple dose response.

### Pioneering of longitudinal pathways is delayed by loss of Gliolectin

The formation of longitudinal pathways is pioneered, in part, by the extension of the pCC and vMP2 axons from each segment towards the next anterior segment (Jacobs and Goodman, 1989a; Jacobs and Goodman, 1989b). Longitudinal extension of these axons is guided by growth cone repulsion from the midline, by positive interactions with laterally positioned intermediate targets (SP1 neurons and longitudinal glia) and by specific fasciculation with posteriorly-extending longitudinal processes (MP1 and dMP2). Several of the cells involved in longitudinal pathfinding are visualized with mAb 1D4 (anti-Fasciclin II), including pCC, vMP2, dMP2, MP1 and SP1 (Goodman and Doe, 1993). Early in longitudinal pathfinding (stage 12/1), the pCC axon does not extend as far anteriorly in  $\Delta 3013$  homozygotes or in *glec*<sup>m98</sup>/ $\Delta 3013$  embryos as in wild type (Fig. 5A,D); rather, it appears stalled after minimal outgrowth (Fig. 5G,J). Later (stage early 13), while the pCC/vMP2 process in wild type has completed its extension to the next segment (Fig. 5B,E), it frequently remains stalled and is often in intimate contact with 1D4-positive midline cells (MP1 and dMP2) in deletion embryos (Fig. 5H). In *glec*<sup>m98</sup>/ $\Delta 3013$  embryos, formation of the pCC/MP1 pathway is severely hampered (Fig. 5K) with few pCC cells

**Table 1. Penetrance and rescue of axon outgrowth phenotypes caused by *Gliectin* loss of function**

Embryonic genotype scored	Phenotype*	Embryos scored	% Embryos affected	Segments scored	% Abnormal segments
OreR (+)	Fused commissure	15	0	170	0
	Delayed longitudinal development	10	10	92	4
$\Delta 3013/+$	Fused commissure	14	7	111	1
	Delayed longitudinal development	7	14	63	2
$\Delta 3013/\Delta 3013$	Fused commissure	23	100	276	64
	Delayed longitudinal development	20	95	234	52
UAS- <i>glec</i> ; <i>rho</i> -Gal4; $\Delta 3013/\Delta 3013$	Fused commissure	8	100	94	31
	Delayed longitudinal development	8	100	88	16
UAS- <i>glec</i> ; UAS- <i>glec</i> / <i>rho</i> -Gal4; $\Delta 3013/\Delta 3013$	Fused commissure	8	25	76	4
	Delayed longitudinal development	6	33	53	6

\*Fused commissure phenotype and delayed longitudinal development were scored at stage 12/1 through early 13.

showing extension beyond the segment of origin. In slightly older  $\Delta 3013$  homozygous embryos (stage late 13), many segments exhibit near normal (Fig. 5C,F) extension of pCC to the next anterior segment (Fig. 5I). However, *glec*<sup>m98</sup>/ $\Delta 3013$  embryos continue to lack a formed pCC/MP1 pathway at this

stage (Fig. 5L). Almost all  $\Delta 3013/\Delta 3013$  embryos (95%) exhibited delayed longitudinal growth in, on average, more than one-half of their segments (Table 1). Longitudinal pathfinding defects were not seen in *glec*<sup>m24</sup>/ $\Delta 3013$  embryos. The segmental broadening observed with mAb BP102 (Fig. 2, Fig. 3) was not apparent with mAb 1D4.

By mid- to late-stage 14, homozygous deletion embryos manifest additional morphological abnormalities that result in significant ventral nerve cord disruptions. In particular, the formation of midgut constrictions is blocked, leading to the generation of a large, poorly organized gut. The appearance of the midgut is identical to that seen in null alleles of *tinman* and *bagpipe*, which lie within the  $\Delta 3013$  interval (Azpiazu and Frasch, 1993). Especially in upper abdominal segments, the midgut mass displaces and fragments the nerve cord, thereby generating both commissural and longitudinal discontinuities (data not shown). However, the axonal phenotypes of younger embryos reported here are distributed evenly across the entire length of the nerve cord and are not clustered in the abdominal segments where gut-induced disruptions are consistently observed by late stage 14. Therefore, as our analysis focuses on stages of development which coincide with the peak of Gliectin expression (stages 12-13) and precede the disruption of gut development (stage 14), we exclude midgut malformation as a cause for the scored axonal phenotypes. In

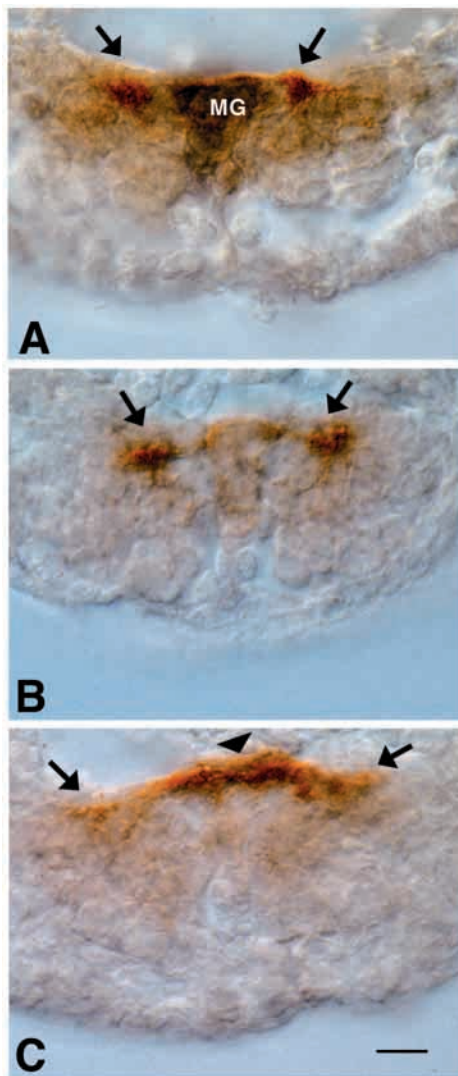


**Fig. 3.** In the absence of Gliectin, commissural axons cross the midline at the dorsal boundary of the nerve cord rather than interdigitating between the midline glial cells. All panels are transverse sections through the ventral nerve cord (20  $\mu$ m, ventral towards the bottom) of stage 12/1 embryos (equivalent to Fig. 2A,F) at the position of maximal commissural axon density. Axons are labeled with mAb BP102 (brown) and the entire width of the nerve cord is presented. (A) Wild-type embryo double stained with mAb 1B7 (black) to visualize the midline glial cells (MG) demonstrates the intimate association between diffuse commissural axons and Gliectin-expressing glial cells. The forming longitudinal comprises a distinct lateral mass of BP102 staining axons (arrows). (B) Without 1B7 staining, the fine distribution of commissural axons between the midline glia is apparent in a wild-type embryo as is the density of fibers in the forming longitudinal (arrows). (C) However, in  $\Delta 3013/\Delta 3013$  embryos, commissural axons fasciculate into a dense bundle that crosses the midline at the dorsal boundary of the nerve cord (arrowhead) and longitudinal mass is greatly reduced (arrows). Scale bar: 5  $\mu$ m.

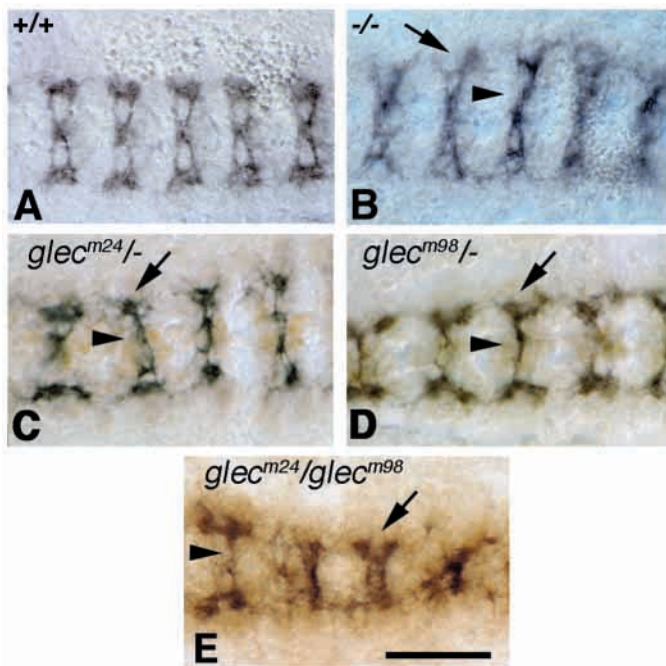


**Fig. 4.** EMS-induced *gliotectin* mutations affect commissure formation. Appearance of commissures stained with mAb BP102 in wild-type embryos (A) and in  $\Delta 3013$  homozygotes (B) at mid-stage 13. Commissure formation is abnormal in the EMS mutant lines designated *glec*<sup>m24</sup> (C) and *glec*<sup>m98</sup> (D) but only when either is in combination with the deletion chromosome ( $\Delta 3013$ ) or with each other (E). Both the *glec*<sup>m24</sup>/ $\Delta 3013$  and *glec*<sup>m98</sup>/ $\Delta 3013$  embryos (C,D) are double-stained with BP102 in black and 1B7 (anti-Gliotectin) in brown, demonstrating that neither mutation abolishes the expression of the Gliotectin antigen. Incomplete commissure separation (B-E, arrowheads) is apparent in the deletion and in the EMS mutants, while decreased longitudinal density is less pronounced in the EMS mutants than in the deletion (B-E, arrows). Scale bar: 13  $\mu$ m.

addition, transgenic rescue of the stage 12-13 axonal phenotype by *rhomboid*-driven Gliotectin expression (see next section) rescued neither the midgut defect nor later stage nerve cord discontinuities. Thus, the effect of genes other than *glec* that are also removed by the  $\Delta 3013$  interval can be dissected away from the Gliotectin null phenotype. For the EMS

hypomorphic alleles *glec*<sup>m24</sup> and *glec*<sup>m98</sup>, similar gut disruptions were not evident in embryos collected from balanced stocks or from crosses to generate either EMS allele in a  $\Delta 3013$  background.

#### Pathfinding defects are rescued by restoration of Gliotectin expression at the midline

To establish that fused commissure and delayed longitudinal phenotypes are attributable to altered *glec* function, Gliotectin was transgenically expressed (UAS-*glec*) at the midline of  $\Delta 3013/\Delta 3013$  embryos under indirect control of the *rhomboid* promoter (*rho*-Gal4). As *rho* is normally activated in cells that also express Gliotectin, *rho*-induced Glec closely reconstitutes wild-type expression (Bier et al., 1990). Although introduction of one copy of the UAS-*glec* transgene did not rescue the embryonic lethality associated with  $\Delta 3013$  homozygosity, it did result in significant improvement in both the commissural organization and longitudinal outgrowth phenotypes (Table 1). Commissural separation is more distinct (Fig. 6A-C) and the intersegmental extension of longitudinal pioneers approaches completion on schedule (Fig. 6E-G, arrow). However, neither phenotype is completely rescued with only one copy of the UAS-*glec* transgene in  $\Delta 3013/\Delta 3013$  embryos. Decreased longitudinal mass (Fig. 6C, arrow) appears more resistant to rescue than commissural fusion (Fig. 6C, arrowhead). A single copy of UAS-*glec* completely rescues the axonal phenotypes of both *glec*<sup>m24</sup>/ $\Delta 3013$  and *glec*<sup>m98</sup>/ $\Delta 3013$  (Table 2) and transgenic Gliotectin expression rescues the lethality of both EMS mutants in the  $\Delta 3013$  background. Construction of  $\Delta 3013/\Delta 3013$  embryos in which a single *rho*-Gal4 element drives expression of Gliotectin from two copies of UAS-*glec* yields nearly complete rescue of delayed longitudinal outgrowth (Fig. 6H, arrow), decreased longitudinal mass (Fig. 6D, arrow) and commissural disorganization (Fig. 6D, arrowhead) associated with the loss-of-function phenotype (Table 1).

Misexpression of Gliotectin protein from a single copy of UAS-*glec* in a wild-type background results in no discernible phenotype. When expressed in all midline cells or in longitudinal glia (*rho*-Gal4), or when driven pan-neurally (*ELAV*-Gal4) or produced by a subset of neurons (*Krüppel*-Gal4) Gliotectin did not affect pioneer axon outgrowth or subsequent fasciculation of follower axons, as assessed by staining with monoclonal antibodies BP102, 1D4 or 22C10 (data not shown).

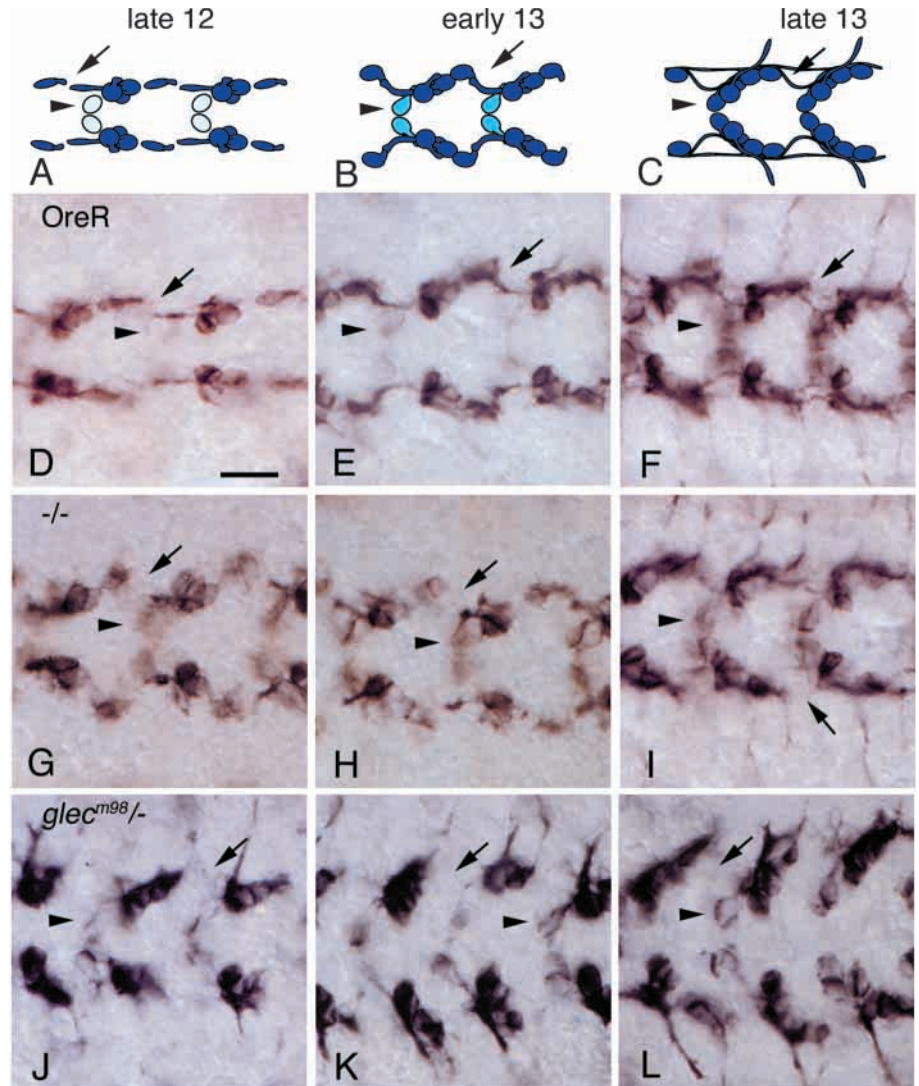
**Table 2. Penetrance and rescue of commissural phenotypes in EMS mutants**

To assess	Cross for embryo collection	Total embryos scored*	% Embryos affected <sup>‡</sup>	Segments scored in affected embryos	% Abnormal segments in affected embryos
<i>glec</i> <sup>m98</sup> / <i>glec</i> <sup>m98</sup>	<i>glec</i> <sup>m98</sup> /TM3 × <i>glec</i> <sup>m98</sup> /TM3	20	0	201	0
<i>glec</i> <sup>m98</sup> / $\Delta 3013$	<i>glec</i> <sup>m98</sup> /TM3 × $\Delta 3013$ /TM6b	45	20	45	78
<i>glec</i> <sup>m98</sup> / $\Delta 3013$ , single copy rescue	UAS- <i>glec</i> ;+; <i>glec</i> <sup>m98</sup> /TM3 × w-; <i>rho</i> -Gal4/ <i>rho</i> -Gal4; $\Delta 3013$ /TM6b	62	8	51	16
<i>glec</i> <sup>m24</sup> / <i>glec</i> <sup>m24</sup>	<i>glec</i> <sup>m24</sup> /TM6b × <i>glec</i> <sup>m24</sup> /TM6b	19	0	197	0
<i>glec</i> <sup>m24</sup> / $\Delta 3013$	<i>glec</i> <sup>m24</sup> /TM6b × $\Delta 3013$ /TM6b	36	25	41	46
<i>glec</i> <sup>m24</sup> / $\Delta 3013$ , single copy rescue	UAS- <i>glec</i> ;+; <i>glec</i> <sup>m24</sup> /TM6b × w-; <i>rho</i> -Gal4/ <i>rho</i> -Gal4; $\Delta 3013$ /TM6b	40	5	25	20

\*Phenotype scored at stage 12/1 through early 13.

<sup>‡</sup>If phenotype is fully penetrant or unrescued, 25% of embryos should be affected in each cross.

**Fig. 5.** Loss of Gliolectin function delays pioneering of the longitudinal pathway. Pioneering of a longitudinal pathway is visualized with the mAb 1D4 (anti-Fasciclin II, nickel-enhanced) in wild-type (A-F),  $\Delta 3013$  homozygous (G-I) and  $glec^{m98}/\Delta 3013$  (J-L) embryos at late stage 12 (A,D,G,J), early stage 13 (B,E,H,K) and late stage 13 (C,F,I,L). In all panels, anterior is towards the left. The schematic diagrams across the top (A-C) depict the progressive completion of the pCC/MP1 pathway. At late stage 12, the pCC growth cone extends anteriorly towards the SP1 neuron (A, in all panels the arrow indicates site at which pCC meets the SP1 neuron). By early stage 13, the pCC growth cone has contacted the SP1 neuron (B, arrow) and continues to grow anteriorly to form a continuous longitudinal pathway by late stage 13 (C, arrow). The intensity of 1D4 staining increases from stage 12 through stage 13 in a pair of neurons at the midline (the dMP2/vMP2 pair, A-L, arrowhead), providing an independent assessment of nerve cord maturation. In the schematic diagram, the level of 1D4 staining is indicated by the shade of blue that colors the dMP2/vMP2 neuron cluster (A-C, arrowhead). In all other panels, the arrowhead indicates the position of the dMP2/vMP2 pair, although only one of these neurons is seen in the relevant focal plane. While dMP2/vMP2 staining is just barely detectable in stage 12 wild-type embryos (A,D, arrowheads), it progressively defines distinct neuronal boundaries by late stage 13 (C,F,I,L, arrowheads). In late stage 13 wild-type embryos, the pCC growth cone displays the streamlined morphology characteristic of a rapidly extending axonal process as it extends towards the point at which it will contact the SP1 neuron (D, arrow). In  $\Delta 3013$  homozygotes at late stage 12, however, pCC axons do not extend as far as in wild type and frequently possess growth cones with spread morphology (G). By early stage 13, pCC frequently remains stalled within its segment of origin and continues to exhibit growth cone morphology more consistent with exploration than with fasciculation in  $\Delta 3013$  homozygotes (H). In late stage 13 deletion homozygotes, pCC has extended into the next segment, although breaks in the pCC/MP1 pathway are frequently seen (I, arrow). In  $glec^{m98}/\Delta 3013$  embryos, the absence of pCC extension is striking (J-L, arrow) even into late stage 13 (L, arrowhead indicates strong staining in vMP2/dMP2, a characteristic of the assigned stage). Scale bar: 5  $\mu$ m in D-L.



## DISCUSSION

### Loss of an endogenous lectin alters the architecture of the *Drosophila* axon scaffold

Gliolectin was originally identified as a *Drosophila* protein that mediates cell adhesion to a subset of N-acetylglucosamine-terminated glycans purified from embryos (Seppo et al., 2000; Tiemeyer and Goodman, 1996). Expressed by midline glial cells in the ventral nerve cord, its spatial and temporal distribution suggested that Gliolectin might participate in axon guidance across the midline. The phenotypes presented here, associated with embryonic loss of Gliolectin, demonstrate that this *Drosophila* carbohydrate-binding protein facilitates the formation of axon-glial contacts. In the absence of Gliolectin, early axon pathway formation across the midline

predominately proceeds through axon extension along other axonal surfaces rather than in close contact with the midline glial cells. The result of growth along this alternative substrate is the formation of a fasciculated bundle of axons that arches over the midline rather than a distributed array of fibers that interdigitates between the midline glia (Fig. 7).

In wild-type embryos, as axons initially extend and cross the midline they are intermixed with many other axons. Some are destined to remain neighbors while others will segregate into different fascicles (Goodman and Shatz, 1993; Simpson et al., 2000a; Simpson et al., 2000b). Signals produced by the midline glia and interpreted by neuronal receptors provide a driving force for axon segregation (Rusch and Van Vactor, 2000). Therefore, maximizing contact between axons and glia would enhance the fidelity of signaling and contribute to sorting

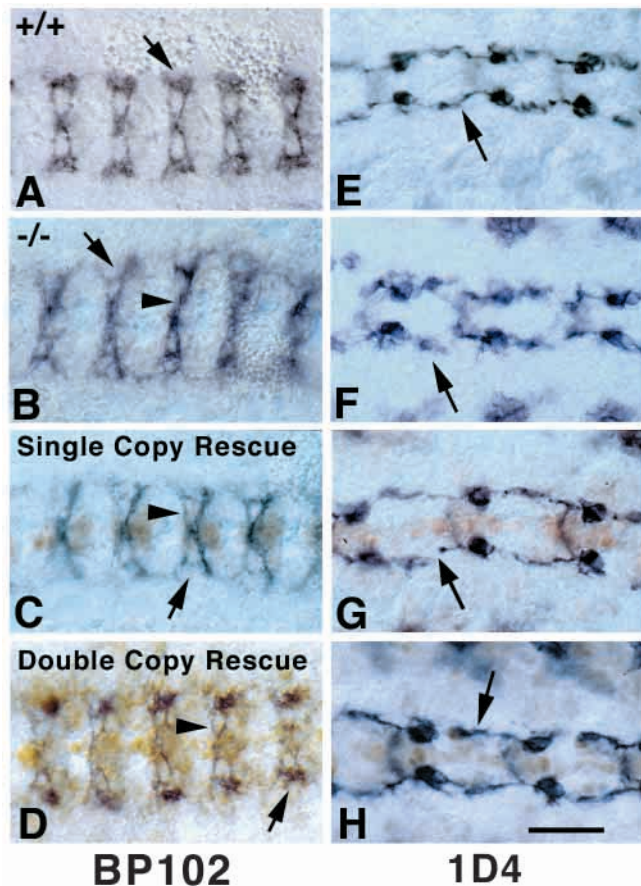


**Fig. 6.** Embryonic CNS phenotypes found in  $\Delta 3013$  homozygotes are rescued by transgenic expression of Gliolectin. Forming commissures are visualized in black with mAb BP102 (A-D, mid-stage 13 embryos) and the pCC longitudinal pioneer is also stained black with mAb 1D4 (E-H, early stage 13 embryos). Compared with wild-type embryos (A,E), commissures and longitudinals are distorted (B, arrowhead and arrow, respectively) and pCC outgrowth is delayed (F, arrow indicates position of SP1 neuron) in  $\Delta 3013$  homozygotes. *rho*-Gal4 driven expression of a single UAS-*glec* element (expression detected with mAb 1B7 in brown in C,D,G,H) partially rescues both the commissural (C, arrowhead) and longitudinal (G) phenotypes of  $\Delta 3013$  homozygotes. In the rescued embryo, commissures are more clearly separated and organized than in the null. Likewise, pCC extension is comparable with wild type; the most severe abnormality observed in rescued embryos is indicated (G, arrow indicates a remaining gap between pCC and SP1 in a single segment). When *rho*-Gal4 drives expression from two copies of UAS-*glec* in a  $\Delta 3013/\Delta 3013$  background, commissures (D, arrowhead) and longitudinals are more completely rescued (arrow in D and H). Scale bar: 12  $\mu$ m in all panels.

mechanisms that operate during transit of axons through the midline. In embryos that lack Gliolectin, the physical separation between extending axons and midline glial surfaces certainly impacts the transmission of sorting signals. While the morphologic probes used in this study do not allow the visualization of inappropriate fasciculation by small subsets of axons, such mis-sorting is implied by the structural alterations observed in the embryonic axon scaffold.

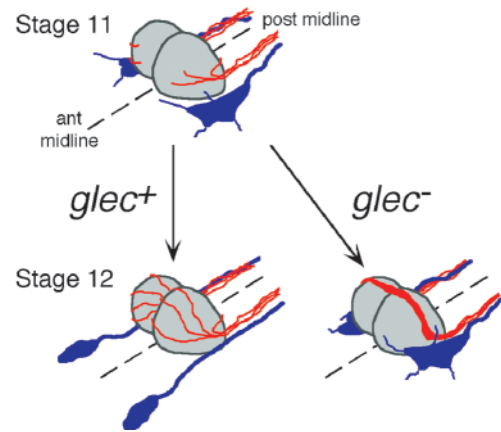


**Fig. 7.** Loss of Gliolectin expression affects commissure and longitudinal formation. Phenotypes associated with loss of Gliolectin indicate that this carbohydrate binding protein functions to capture axons at the surface of the midline glial cells (shown in gray) in which it is expressed. For longitudinal axons (shown in blue), capture facilitates the transmission of signals that keep them from crossing the midline (Robo, Slit). In the absence of Gliolectin, longitudinal axon extension is delayed. For commissural axons (shown in red), capture ensures the transmission of signals that allow midline crossing (Commissureless, Netrins) and contributes to the formation of a favorable growth substrate. In the absence of Gliolectin, early commissural axons grow upon other axons rather than in close association with the midline glia.

### Loss of Gliolectin affects the efficiency of midline signal transmission

Axons that pioneer longitudinal pathways, such as the axon of the pCC neuron, are normally retained on the ipsilateral side of the nerve cord by repulsive signals expressed by the midline glia. Interactions between Slit, a midline glial protein, and neuronal Roundabout (Robo) receptors maintain longitudinal axon growth in an anterior-posterior trajectory by causing the withdrawal of nascent contacts between longitudinal axons and the midline. Faced with a formidable inhibitory environment at the midline, susceptible axons efficiently extend along more favorable longitudinal routes. In the absence of repulsive signaling components (either Slit or Robo), axons normally destined to remain in the longitudinals instead freely cross the midline, indicating that the midline possesses an underlying substrate favorable for axon growth (Kidd et al., 1999; Kidd et al., 1998a; Rajagopalan et al., 2000).

In the absence of Gliolectin, we find that midline repulsion of longitudinal axons is not abolished. However, as demonstrated by the behavior of the pCC axon, the efficiency of the repulsive response is reduced. We observe that the pCC axon is delayed in its anterior course, frequently exhibiting extended interactions with what are usually transient substrates (Fig. 7). Such aberrant behavior indicates that Gliolectin normally provides sufficient contact between midline glia and filipodial extensions to ensure efficient repulsive signal transmission. Therefore, the observed *glec*<sup>-</sup> phenotype predicts that partially penetrant midline-crossing defects associated with *robo* hypomorphic alleles should be enhanced by a concomitant reduction in Gliolectin.

Axons that pioneer commissural pathways normally extend

through the midline by ignoring repulsive signals (Seeger et al., 1993). The activity of the Commissureless (Comm) protein, another midline glial protein, instructs a subset of axons to downregulate Robo receptors and consequently disregard Slit (Tear et al., 1996). Loss of the Commissureless protein results in loss of commissures because axons are uniformly repelled from the midline. However, despite loss of this inhibitor of repulsion, axons initially orient towards and probably also adhere to the midline glia (as these cells are laterally displaced in some *comm* mutant alleles). Adhesion, or at least intimate contact, between presumptive commissural axons and the midline glia is also implicit in the proposal that Comm signaling proceeds through the transcellular transfer of Commissureless transmembrane protein from midline glial cell to axon (Tear et al., 1996).

As loss of Gliolectin affects the extent of physical contact between axons and midline glial cells (Fig. 7), minimal Commissureless signaling would be expected in *glec*<sup>-</sup> mutants. Therefore, loss of Gliolectin should enhance hypomorphic *comm* alleles by attenuating residual signaling. Furthermore, as axon commissures are present, although distorted, in *glec*<sup>-</sup> embryos, it is once again apparent that loss of Gliolectin affects the fidelity of axon fasciculation and not the absolute specificity of pathfinding. In the absence of the adhesivity provided by Gliolectin-carbohydrate interactions, the amount of signaling passed between the midline glia and a neuronal growth cone is controlled solely by the duration of chance filipodial contact. Gliolectin functions, therefore, as a capture mechanism that ensures neural and glial membranes remain in contact long enough to communicate and integrate relevant sorting information. Recently, an adult bristle phenotype was described in an EP line possessing an Enhancer/Promoter P-element insertion into the *glec* locus, suggesting that in other contexts Gliolectin may also facilitate cell signaling (Abelilah-Seyfried et al., 2000).

### Gliolectin function is consistent with other carbohydrate-mediated interactions

In several contexts, carbohydrate-binding proteins and their recognized ligands provide a mechanism for capture at specific tissue sites. For example, the Selectin family of C-type lectins and their carbohydrate ligands are expressed on leukocytes, platelets and endothelial cells where they mediate the initial interactions between inflammatory cells and specialized endothelial domains in vertebrate vasculature (Tiemeyer et al., 1991; Whelan, 1996). Circulating lymphocytes are recruited to sites of endothelial inflammation by the interaction between a lymphocyte-expressed selectin (L-Selectin) and appropriate endothelial cell carbohydrate ligands (primarily oligosaccharides bearing a sialyl-Lewis<sup>X</sup> structure). Engagement of sufficient selectin-ligand pairs induces lymphocytes to roll along the endothelium, thus allowing additional signaling and adhesive interactions to generate subsequent cellular extravasation (Springer, 1994). At the outset of this process, it is the presence of a carbohydrate-mediated capture mechanism that ensures the efficiency and localization of the inflammatory response.

As loss of selectin-mediated interactions abolishes leukocyte extravasation while loss of Gliolectin does not completely abolish normal axon sorting, the parallels between selectin-mediated whole cell capture and Gliolectin-mediated axon

capture are not absolute (Maly et al., 1996). Selectins, however, operate under conditions of hydrodynamic flow where cells are quickly swept away if not captured. The environment in which Gliolectin operates is more static; extending axons reside in appropriate regions of the developing nerve cord long enough to heed available signals, despite the loss of intimate glial contact. Under these conditions, loss of Gliolectin affects only the efficiency not the direction of axon pathfinding. Nonetheless, the important characteristic shared by Gliolectin- and Selectin-mediated carbohydrate binding is that they constitute the initial step in a process that leads to subsequent cellular responses (Lasky, 1992; Lasky, 1995).

For longitudinal axons, this response is withdrawal from the midline. For commissural axons, the response to Gliolectin-mediated contact is to maximize contact with midline glial cells at the expense of axon-axon contact. Gliolectin, then, provides a permissive substrate for commissural axon segregation. Similarly, in the vertebrate embryonic nervous system, regulated expression of an anionic carbohydrate polymer, poly- $\alpha$ 2,8-linked sialic acid, facilitates segregation of motor axons into functionally related fascicles (Acheson et al., 1991; Stoeckli et al., 1997). Furthermore, the fidelity of axon fasciculation in developing invertebrate nervous systems is affected both by altered glycan expression and by glycan-directed biochemical perturbations (Song and Zipser, 1995; Whitlock, 1993). While these glycan-mediated axon segregation events have not been shown to require a carbohydrate-lectin interaction, they nevertheless demonstrate the importance of regulated carbohydrate expression and oligosaccharide function in axon sorting.

### Carbohydrate-mediated axon capture functions within a hierarchy of activities to ensure appropriate axon pathfinding

It was first suggested over 30 years ago that carbohydrate-protein interactions might impart specificity to cell-cell interactions (Roseman, 1970). The nervous system, which is particularly rich and varied in its glycan expression, has historically served as a hunting ground for signs of carbohydrate-mediated cell-cell recognition, especially during development. Characterization of the diversity and intricacy of neural cell-specific glycan expression continues to expand. However, a corresponding range of endogenous neural lectins with the capacity to interpret the cell-surface carbohydrate code has yet to be described. Although perhaps simply reflecting the relative paucity of genetic and molecular analysis applied to carbohydrate function, this deficiency also reinforces the suggestion that specificity is primarily an emergent property of the interdependent activities of multiple genes. Even though Gliolectin function is necessary to efficiently initiate a cascade that results in specific pathfinding, axon capture by itself does not guarantee appropriate growth cone response. Likewise, normal signaling in the absence of axon capture yields imperfect fasciculation.

Thus, on top of regulated signaling molecule and receptor function, the embryonic nervous system overlays appropriate spatial and temporal expression patterns of lectin-ligand pairs to ensure high-fidelity axon pathfinding. Estimating the total number of lectin-ligand pairs relevant to *Drosophila* embryonic development would be excessively speculative even with completion of the genome sequence (Dodd and Drickamer,

2001; Drickamer and Dodd, 1999; Seppo and Tiemeyer, 2000; Theopold et al., 1999). However, by wedding signaling specificity to carbohydrate-mediated capture, the need for stringent recognition markers is reduced. Additionally, if non-interacting cells effectively ignore locally proffered signals, a small number of moderately discriminate adhesion molecules would reduce the level of specificity required of signaling mechanisms. The composite effect, then, of carbohydrate-mediated axon capture would be to sharpen the sphere of influence of combinatorial signaling codes and thus impart greater specificity to axon pathfinding.

We thank Corey Goodman for supplying antibodies and advice. We also thank Liva Andreeva for generating UAS-*glec* insertion lines and Iris Bonilla, Richard Hsu and Katherine Parisky for their contributions to early aspects of this project. Carl Hashimoto, Lynn Cooley and members of their respective laboratories provided support and useful suggestions. Grant support from the NIH-NICD (HD33878), from the March of Dimes (Basil O'Connor Award) and from the Patrick and Catherine Weldon Donaghue Foundation (all to M. T.) is gratefully acknowledged. M. S. received support from NIH-NIGMS (GM07223).

## REFERENCES

- Abdelilah-Seyfried, S., Chan, Y-M, Zeng, C., Justice, N. J., Younger-Shepherd, S., Sharp, L. C., Barbel, S., Meadows, S. A., Jan, L. Y. and Jan, Y. N. (2000). A gain-of-function screen for genes that affect the development of the *Drosophila* adult external sensory organ. *Genetics* **155**, 733-752.
- Acheson, A., Sunshine, J. L. and Rutishauser, U. (1991). NCAM polysialic acid can regulate both cell-cell and cell-substrate interactions. *J. Cell Biol.* **114**, 143-153.
- Azpiazuz, N. and Frasch, M. (1993). *tinman* and *bagpipe*: two homeo box genes that determine cell fates in the dorsal mesoderm of *Drosophila*. *Genes Dev.* **7**, 1325-1340.
- Bier, E., Jan, L. Y. and Jan, Y. N. (1990). *Rhomboid*, a gene required for dorsoventral axis establishment and peripheral nervous system development in *Drosophila melanogaster*. *Genes Dev.* **4**, 190-203.
- Bovolenta, P. and Mason, C. (1987). Growth cone morphology varies with position in the developing mouse visual pathway from retina to first targets. *J. Neurosci.* **7**, 1447-1460.
- Brand, A. H., Manoukian, A. S. and Perrimon, N. (1994). Ectopic Expression in *Drosophila*. In *Drosophila melanogaster: Practical Uses in Cell and Molecular Biology*. Vol. 44 (ed. L. S. B. Goldstein and E. Fyrberg), pp. 635-654. San Diego: Academic Press.
- Callaerts, P., Vulsteke, V., Peumans, W. and De, L. A. (1995). Lectin binding sites during *Drosophila* embryogenesis. *Roux's Arch. Dev. Biol.* **204**, 229-243.
- Campos-Ortega, J. A. and Hartenstein, V. (1997). In *The Embryonic Development of Drosophila melanogaster*. pp. 3-84. Berlin: Springer-Verlag.
- D'Amico, P. and Jacobs, J. R. (1995). Lectin histochemistry of the *Drosophila* embryo. *Tissue Cell* **27**, 23-30.
- Dodd, R. B. and Drickamer, K. (2001). Lectin-like proteins in model organisms: implications for evolution of carbohydrate-binding activity. *Glycobiology* **11**, 71R-79R.
- Drickamer, K. and Dodd, R. B. (1999). C-type lectin-like domains in *Caenorhabditis elegans*: predictions from the complete genome sequence. *Glycobiology* **9**, 1357-1369.
- Fredieu, J. R. and Mahowald, A. P. (1994). Glycoconjugate expression during *Drosophila* embryogenesis. *Acta Anat.* **149**, 89-99.
- Fristrom, D. K. and Fristrom, J. W. (1982). Cell surface binding sites for peanut agglutinin in the differentiating eye disc of *Drosophila*. *Dev. Biol.* **92**, 418-427.
- Goodman, C. S. and Doe, C. Q. (1993). Embryonic development of the *Drosophila* central nervous system. In *The Development of Drosophila melanogaster* (ed. M. Bate and A. M. Arias), pp. 1131-1206. Cold Spring Harbor: Cold Spring Harbor Laboratory Press.
- Goodman, C. S. and Shatz, C. J. (1993). Developmental mechanisms that generate precise patterns of neuronal connectivity. *Cell* **72 Suppl.**, 77-98.
- Harris, R., Sabatelli, L. M. and Seeger, M. A. (1996). Guidance cues at the *Drosophila* CNS midline: identification and characterization of two *Drosophila* Netrin/UNC-6 homologs. *Neuron* **17**, 217-228.
- Hummel, T., Schimmelpfeng, K. and Klämbt, C. (1999). Commissure formation in the embryonic CNS of *Drosophila*. *Development* **126**, 771-779.
- Hummel, T., Leifker, K. and Klämbt, C. (2000). The *Drosophila* HEM-2/NAP1 homolog KETTE controls axonal pathfinding and cytoskeletal organization. *Genes Dev.* **14**, 863-873.
- Isbister, C. M., Tsai, A., Wong, S. T., Kolodkin, A. L. and O'Connor, T. P. (1999). Discrete roles for secreted and transmembrane semaphorins in neuronal growth cone guidance in vivo. *Development* **126**, 2007-2019.
- Jacobs, J. R. and Goodman, C. S. (1989a). Embryonic development of axon pathways in the *Drosophila* CNS. I. A glial scaffold appears before the first growth cones. *J. Neurosci.* **9**, 2402-2411.
- Jacobs, J. R. and Goodman, C. S. (1989b). Embryonic development of axon pathways in the *Drosophila* CNS. II. Behavior of pioneer growth cones. *J. Neurosci.* **9**, 2412-2422.
- Kidd, T., Brose, K., Mitchell, K. J., Fetter, R. D., Tessier-Lavigne, M., Goodman, C. S. and Tear, G. (1998a). Roundabout controls axon crossing of the CNS midline and defines a novel subfamily of evolutionarily conserved guidance receptors. *Cell* **92**, 205-215.
- Kidd, T., Russell, C., Goodman, C. S. and Tear, G. (1998b). Dose-sensitive and complementary functions of Roundabout and Commissureless control axon crossing of the CNS midline. *Neuron* **20**, 25-33.
- Kidd, T., Bland, K. S. and Goodman, C. S. (1999). Slit is the midline repellent for the robo receptor in *Drosophila*. *Cell* **96**, 785-794.
- Klämbt, C. and Goodman, C. S. (1991a). The diversity and pattern of glia during axon pathway formation in the *Drosophila* embryo. *Glia* **4**, 205-213.
- Klämbt, C. and Goodman, C. S. (1991b). Role of the midline glia and neurons in the formation of the axon commissures in the central nervous system of the *Drosophila* embryo. *Ann. New York Acad. Sci.* **633**, 142-159.
- Klämbt, C., Jacobs, J. R. and Goodman, C. S. (1991). The midline of the *Drosophila* central nervous system: a model for the genetic analysis of cell fate, cell migration, and growth cone guidance. *Cell* **64**, 801-815.
- Kolodkin, A. L., Matthes, D. J., O'Connor, T. P., Patel, N. H., Admon, A., Bentley, D. and Goodman, C. S. (1992). Fasciclin IV: sequence, expression, and function during growth cone guidance in the grasshopper embryo. *Neuron* **9**, 831-845.
- Landmesser, L., Dahm, L., Tang, J. and Rutishauser, U. (1990). Polysialic acid as a regulator of intramuscular nerve branching during embryonic development. *Neuron* **4**, 655-667.
- Lasky, L. (1992). Selectins: interpreters of cell-specific carbohydrate information during inflammation. *Science* **258**, 946-969.
- Lasky, L. A. (1995). Selectin-carbohydrate interactions and the initiation of the inflammatory response. *Annu. Rev. Biochem.* **64**, 113-139.
- Lewis, E. B. and Bacher, F. (1988). Method of feeding ethyl methane sulfonate (EMS) to *Drosophila* males. *Drosophila Information Service* **43**, 193.
- Maly, P., Thall, A. D., Petryniak, B., Rogers, C. E., Smith, P. L., Marks, R. M., Kelly, R. J., Gersten, K. M., Cheng, G., Camphausen, R. T. et al. (1996). The  $\alpha(1,3)$ fucosyltransferase Fuc-TVII controls leukocyte trafficking through an essential role in L-, E- and P-selectin ligand biosynthesis. *Cell* **86**, 643-653.
- Marcus, R. C., Blazeski, R., Godement, P. and Mason, C. A. (1995). Retinal axon divergence in the optic chiasm: Uncrossed axons diverge from crossed axons within a midline glial specialization. *J. Neurosci.* **15**, 3716-3729.
- Patel, N. H. (1994). Imaging neuronal subsets and other cell types in whole mount *Drosophila* embryos and larvae using antibody probes. In *Drosophila melanogaster: Practical Uses in Cell and Molecular Biology*. Vol. 44 (ed. L. S. B. Goldstein and E. Fyrberg), pp. 445-487. San Diego: Academic Press.
- Rajagopalan, S., Nicolas, E., Vivancos, V., Berger, J. and Dickson, B. J. (2000). Crossing the midline: Roles and regulation of Robo receptors. *Neuron* **28**, 767-777.
- Rietveld, A., Neutz, S., Simons, K. and Eaton, S. (1999). Association of sterol- and glycosylphosphatidylinositol-linked proteins with *Drosophila* raft lipid microdomains. *J. Biol. Chem.* **274**, 12049-12054.
- Roseman, S. (1970). The synthesis of complex carbohydrates by multiglycosyltransferase systems and their potential function in intercellular adhesion. *Chem. Phys. Lipids* **5**, 270-297.
- Roth, J., Kempf, A., Reuter, G., Schauer, R. and Gehring, W. J. (1992).

- Occurrence of sialic acids in *Drosophila melanogaster*. *Science* **256**, 673-675.
- Rusch, J. and Van Vactor, D.** (2000). New roundabouts send axons into the fas lane. *Neuron* **28**, 637-640.
- Seeger, M., Tear, G., Ferres-Marco, D. and Goodman, C. S.** (1993). Mutations affecting growth cone guidance in *Drosophila*: genes necessary for guidance toward or away from the midline. *Neuron* **10**, 409-426.
- Seppo, A., Moreland, M., Schweingruber, H. and Tiemeyer, M.** (2000). Zwitterionic and acidic glycosphingolipids of the *Drosophila melanogaster* embryo. *Eur. J. Biochem.* **267**, 3549-3558.
- Seppo, A. and Tiemeyer, M.** (2000). Function and structure of *Drosophila* glycans. *Glycobiology* **10**, 751-760.
- Simpson, J. H., Bland, K. S., Fetter, R. D. and Goodman, C. S.** (2000a). Short-range and long-range guidance by Slit and its Robo receptors: A combinatorial code of Robo receptors controls lateral position. *Cell* **103**, 1019-1032.
- Simpson, J. H., Kidd, T., Bland, K. S. and Goodman, C. S.** (2000b). Short-range and long-range guidance by Slit and its Robo receptors: Robo and Robo2 play distinct roles in midline guidance. *Neuron* **28**, 753-766.
- Song, J. and Zipser, B.** (1995). Targeting of neuronal subsets mediated by their sequentially expressed carbohydrate markers. *Neuron* **14**, 537-547.
- Springer, T. A.** (1994). Traffic signals for lymphocyte recirculation and leukocyte emigration: The multistep paradigm. *Cell* **76**, 301-314.
- Stein, E. and Tessier-Lavigne, M.** (2001). Hierarchical organization of guidance receptors: silencing of Netrin attraction by Slit through a robo/DCC receptor complex. *Science* **291**, 1928-1938.
- Stoeckli, E. T. and Landmesser, L. T.** (1998). Axon guidance at choice points. *Curr. Opin. Neurobiol.* **8**, 73-79.
- Stoeckli, E. T., Sonderegger, P., Pollerberg, G. E. and Landmesser, L. T.** (1997). Interference with axonin-1 and NrCAM interactions unmasks a floor-plate activity inhibitory for commissural axons. *Neuron* **18**, 209-221.
- Tear, G., Harris, R., Sutaria, S., Kilomanski, K., Goodman, C. S. and Seeger, M. A.** (1996). *commissureless* controls growth cone guidance across the CNS midline in *Drosophila* and encodes a novel membrane protein. *Neuron* **16**, 501-514.
- Theopold, U., Rissler, M., Fabbri, M., Schmidt, O. and Natori, S.** (1999). Insect glycobiology: A lectin multigene family in *Drosophila melanogaster*. *Biochem. Biophys. Res. Commun.* **261**, 923-927.
- Tiemeyer, M. and Goodman, C. S.** (1996). Gliolectin is a novel carbohydrate-binding protein expressed by a subset of glia in the embryonic *Drosophila* nervous system. *Development* **122**, 925-36.
- Tiemeyer, M., Swieder, S. J., Ishihara, M., Moreland, M., Schweingruber, H., Hirtzer, P. and Brandley, B. K.** (1991). Carbohydrate ligands for endothelial-leukocyte adhesion molecule 1. *Proc. Natl. Acad. Sci* **88**, 1138-1142.
- Toyoda, H., Kinoshita-Toyoda, A. and Selleck, S. B.** (2000). Structural analysis of glycosaminoglycans in *Drosophila* and *Caenorhabditis elegans* and demonstration that *tout-velu*, a *Drosophila* gene related to EXT tumor suppressors, affects heparan sulfate in vivo. *J. Biol. Chem.* **375**, 2269-2275.
- Whelan, J.** (1996). Selectin synthesis and inflammation. *Trends Biochem. Sci.* **21**, 65-69.
- Whitlock, K. E.** (1993). Development of *Drosophila* wing sensory neurons in mutants with missing or modified cell surface molecules. *Development* **117**, 1251-1260.
- Winberg, M. L., Mitchell, K. J. and Goodman, C. S.** (1998). Genetic analysis of the mechanisms controlling target selection: complementary and combinatorial functions of netrins, semaphorins, and IgCAMs. *Cell* **93**, 581-591.